



# Combined negative effect of donor age and time in culture on the reprogramming efficiency into induced pluripotent stem cells

Ras Trokovic<sup>a,1</sup>, Jere Weltner<sup>a,1</sup>, Parinya Noisa<sup>b,c</sup>,  
Taneli Raivio<sup>b,d</sup>, Timo Otonkoski<sup>a,d,\*</sup>

<sup>a</sup> Research Programs Unit, Molecular Neurology, Biomedicum Stem Cell Center, University of Helsinki, Helsinki, Finland

<sup>b</sup> Institute of Biomedicine, Department of Physiology, University of Helsinki, Helsinki, Finland

<sup>c</sup> School of Biotechnology, Institute of Agricultural Technology, Suranaree University of Technology, Nakhon Ratchasima, Thailand

<sup>d</sup> Children's Hospital, Helsinki University Hospital and University of Helsinki, Helsinki, Finland

Received 30 April 2014; received in revised form 1 June 2015; accepted 5 June 2015

Available online 11 June 2015

## Abstract

Somatic cells can be reprogrammed into induced pluripotent stem cells (iPSC) by the forced expression of the transcription factors OCT4, SOX2, KLF4 and c-MYC. Pluripotent reprogramming appears as a slow and inefficient process because of genetic and epigenetic barriers of somatic cells. In this report, we have extended previous observations concerning donor age and passage number of human fibroblasts as critical determinants of the efficiency of iPSC induction. Human fibroblasts from 11 different donors of variable age were reprogrammed by ectopic expression of reprogramming factors. Although all fibroblasts gave rise to iPSC colonies, the reprogramming efficiency correlated negatively and declined rapidly with increasing donor age. In addition, the late passage fibroblasts gave less reprogrammed colonies than the early passage cell counterparts, a finding associated with the cellular senescence-induced upregulation of p21. Knockdown of p21 restored iPSC generation even in long-term passaged fibroblasts of an old donor, highlighting the central role of the p53/p21 pathway in cellular senescence induced by both donor age and culture time.

© 2015 The Authors. Published by Elsevier B.V. This is an open access article under the CC BY-NC-ND license (<http://creativecommons.org/licenses/by-nc-nd/4.0/>).

## Introduction

Reprogramming rejuvenates aged somatic cells back into the pluripotent state (Takahashi et al., 2007; Takahashi and

Yamanaka, 2006). The developmental plasticity of induced pluripotent stem cells (iPSC) demonstrated the potential for regenerative therapies of human diseases (Braam et al., 2013; Song et al., 2012; Yu et al., 2012). Various types

DOIs of original article: <http://dx.doi.org/10.1016/j.scr.2015.05.012>, <http://dx.doi.org/10.1016/j.scr.2015.05.013>.

\* Corresponding author at: Research Programs Unit, Molecular Neurology, Biomedicum Stem Cell Center, University of Helsinki, Biomedicum Helsinki, PO Box 63 (Haartmaninkatu 8), 00014 Helsinki, Finland.

E-mail addresses: [ras.trokovic@helsinki.fi](mailto:ras.trokovic@helsinki.fi) (R. Trokovic), [jere.weltner@helsinki.fi](mailto:jere.weltner@helsinki.fi) (J. Weltner), [p.noisa@sut.ac.th](mailto:p.noisa@sut.ac.th) (P. Noisa), [taneli.raivio@helsinki.fi](mailto:taneli.raivio@helsinki.fi) (T. Raivio), [timo.otonkoski@helsinki.fi](mailto:timo.otonkoski@helsinki.fi) (T. Otonkoski).

<sup>1</sup> These authors contributed equally to this work.

<http://dx.doi.org/10.1016/j.scr.2015.06.001>

1873-5061/© 2015 The Authors. Published by Elsevier B.V. This is an open access article under the CC BY-NC-ND license (<http://creativecommons.org/licenses/by-nc-nd/4.0/>).

of somatic cells have been successfully used for iPSC derivation, including for instance skin fibroblasts, blood cells and myoblasts (Seki et al., 2010; Trokovic et al., 2013, 2014; Yu et al., 2007). Alternative methods for iPSC derivation have been intensively developed to avoid the integration of transgenes, including reprogramming induced by Sendai virus, mRNA, episomal vectors or small molecules (Hou et al., 2013; Nishimura et al., 2011; Warren et al., 2010; Zhou et al., 2009). Although methods for iPSC derivation have been intensively developed, most current technologies are still inefficient, which may be due to intrinsic barriers in the ability of cells to undergo a rapid shift in their proliferative rate (Hanna et al., 2009; Smith et al., 2010).

Multiple factors are known to contribute to the efficiency of iPSC generation (Park et al., 2014). For example, differentiation state of the starting cell is a significant factor, since progenitors and stem cells give higher reprogramming efficiency than terminally differentiated cells (Eminli et al., 2009). There is also evidence for varying efficiency for different types of somatic cells from the same donor (Streckfuss-Bomeke et al., 2013). In addition cellular senescence has been shown to affect the reprogramming efficiency (Banito et al., 2009; Kawamura et al., 2009; Li et al., 2009; Marión et al., 2009; Utikal et al., 2009). Cellular senescence increases with age and one of its hallmarks is the irreversible cell cycle arrest through the activation of the p53/p21 and p16 pathways (Campisi and d'Adda di Fagagna, 2007; Narita et al., 2003). These findings suggest that intrinsic properties of somatic cells determine the reprogramming efficiency.

Donor age has been shown to have an effect on reprogramming efficiency of murine cells (Wang et al., 2011). Contrary to what has been observed in mice, donor age was suggested not to impair the reprogramming efficiency of human cells (Somers et al., 2010) and iPSC have been successfully derived even from the fibroblasts of centenarians (Lapasset et al., 2011). However, there are no reports on the combined effect of age and culture time on reprogramming efficiency of human cells.

The aim of this report was to evaluate the independent and combined impact of donor age and passage number on the pluripotent reprogramming efficiency of human dermal fibroblasts. Gene expression profiles of selected genes and telomere lengths of starting fibroblasts were analyzed in order to identify potential factors behind distinct reprogramming efficiencies. We found that the reprogramming efficiency of human dermal fibroblasts is synergistically affected by donor age and culture time, both inducing cellular senescence through the p53/p21 pathway.

## Materials and methods

### Ethics, description of the human material

Donors or their guardians provided their written informed consent for participation. Coordinating Ethics Committee of Helsinki and Uusimaa Hospital District approved generation and use of human iPSC (statement nr. 423/13/03/00/08) on April 2009. Human dermal fibroblasts and foreskin fibroblasts (HFF; CRL-2429; ATCC) were used for reprogramming (Table 1).

**Table 1** Information on donors of fibroblasts used in this study.

Donor nr	Cell type	Age at biopsy (yr)	Sex	Diagnosis
1	Foreskin fibroblast	0	Male	Healthy (ATCC)
2	Skin fibroblast	1	Female	PNDM
3	Skin fibroblast	14	Female	PNDM
4	Skin fibroblast	18	Male	PNDM
5	Skin fibroblast	22	Female	Healthy
6	Skin fibroblast	32	Female	PNDM
7	Skin fibroblast	43	Female	Healthy
8	Skin fibroblast	49	Male	Healthy
9	Skin fibroblast	57	Female	Healthy
10	Skin fibroblast	81	Male	Healthy
11	Skin fibroblast	83	Male	Healthy

PNDM, Permanent Neonatal Diabetes Mellitus.

### Cell culture and fibroblasts reprogramming

Human foreskin fibroblasts (CRL-2429, ATCC) and dermal fibroblasts that were derived from skin biopsies were cultured in DMEM (Sigma) supplemented with 10% FBS (Life Technologies) and GlutaMAX (Life Technologies) (Table 1). Human induced pluripotent stem cells were cultured in hESC medium: DMEM/F12 with GlutaMAX (Life Technologies), 10% knockout serum replacement (Life Technologies), 0.1 mM 2-mercapthoethanol (Life Technologies), 1× non-essential amino acids (Life Technologies), and 6 ng/ml bFGF (Sigma) or E8 (Life Technologies) on matrigel and routinely propagated with combination of collagenase IV treatment and mechanic dissociation. Fibroblasts were reprogrammed using four Yamanaka factors (OCT4, SOX2, KLF4, and C-MYC) using pMXs retroviruses or Sendai viruses: SeV (Cytotune; Life Technologies), or SeVdp (Nishimura et al., 2011) on matrigel and E6 medium (Life Technologies) and as described previously (Hussein et al., 2011; Trokovic et al., 2013, 2014).

To enhance the reprogramming of fibroblasts 0.25 mM sodium butyrate (NaB; Sigma, B5887) was added to all reprogramming experiments. In order to rescue cells from senescence siRNA targeting human *CDKN1A* (p21) was obtained from Dharmacon (M-003471-00-0005). Daily transfections were performed using 10 pmol siRNA with Lipofectamine RNAiMAX Reagent (Life Technologies). siRNA was administered on the daily basis in duration of 20 days, starting five days prior Sendai virus infection. To show that an increase in p21 expression reduces reprogramming efficiency, p21 followed by puromycin N-acetyl-transferase (PAC) was cloned into pMXs vector and added to the reprogramming cocktail. As a control pMXs\_EGFP\_PAC vector was used. To ensure that all fibroblasts contained vectors with p21 or EGFP, we added puromycin to the media for the duration of reprogramming.

### Immunocytochemistry and alkaline phosphatase staining

Cells were fixed at room temperature with 4% paraformaldehyde for 10 min. Non-specific proteins were blocked by ultra V block (Thermo). The cells were then treated with primary antibodies overnight at 4 °C. Primary antibodies

were against TRA-1-60 (1:500, MA1-023, Thermo Fisher), OCT4 (1:500, C30A3, Cell Signaling), SSEA3 (1:100, MAB4303, Millipore). After washing with PBS, the cells were incubated with fluorescence-conjugated secondary antibody AlexaFluor 488: donkey anti-goat (1:500, A11055, Life Technologies), goat anti-mouse (1:500, A21042, Life Technologies), and goat anti-rat (1:500, A21212, Life Technologies) for 45 min, and finally mounted to the cover-slip with Vectashield mounting medium with DAPI (Vectorlabs). Alkaline-phosphatase (AP) was detected using NBT/ BCIP solution (Roche Applied Science).

For live cell staining the cells were incubated with primary antibody against TRA-1-60 (1:50, MA1-023, Thermo Fisher) and fluorescence-conjugated secondary antibody AlexaFluor 488 goat anti-mouse (1:50, A21042, Life Technologies) for 1 h at 37 °C and 5% CO<sub>2</sub> and visualized under the EVOS fluorescence microscope (Life Technologies).

### Western blotting

Cell samples for protein analysis were collected from confluent 6 cm dishes and cell pellets were resuspended in RIPA buffer. Protein amounts were measured from the supernatant using Protein Quantification Assay (Macherey & Nagel). 40 µg of protein per sample was used for SDS-PAGE. Proteins were transferred onto nitrocellulose membranes using iBlot dry blotting system (Life Technologies). Membranes were blocked with TBST + 5% milk powder and p21 primary antibody incubations were made overnight. HRP-conjugated secondary antibodies were incubated in room temperature for 1 h. Proteins were detected using Amersham ECL Prime Western Blotting Detection Reagent (GE healthcare). The following antibodies were used: mouse anti-p21 (556431, Pharmingen, 1:500), Actin-HRP (sc-1616 HRP, Santa Cruz, 1:2000), anti-mouse HRP (7076P2, Cell Signaling, 1:2000).

### Teratoma formation

About 200,000 morphologically intact iPSC were intratesticularly injected into male NMRI nude mice (Scanbur). The resulting tumors were collected 8 weeks after injection, fixed with 10% formalin, and hematoxylin and eosin stained. The experimental animal welfare committee of the District Government of Southern Finland approved the animal experiments.

### Reverse transcription and quantitative PCR (qPCR)

Total RNA was extracted using RNA Spin II (Macherey-Nagel) by following the manufacturer's instructions. Briefly, first-strand cDNA was synthesized from 2 µg total RNA by SuperScript III reverse transcriptase (Invitrogen) with oligo dT primer (Invitrogen) in 20 µl volume. 1% of above cDNA was used for each qPCR reaction in a 20 µl mixture containing 10 µl of SYBR green-Taq mixed solution (Sigma) and 5 µl of 2 µM-primer mix. PCR reactions were carried out in a Corbette thermal cycler (Qiagen) for 40 cycles and each cycle contained 95 °C for 15 s, 60 °C for 30 s and 72 °C for 30 s. RNA without reverse transcription was used as a negative control. The relative expression level of genes was calculated by calibrating their CT values with that of the housekeeping gene *Cyclophilin G*,

and normalized to fibroblasts at passage 6 (as reference sample). List of primers is provided in Supplementary Table 1.

### Telomere measurement

DNA was isolated from fibroblasts by genomic DNA extraction kit (Invitrogen) for telomere measurement. Telomere length was measured as previously described (Cawthon, 2002) by qPCR amplification with oligonucleotide primers designed to hybridize to the TTAGGG and CCCTAA repeats. For all qPCR reactions, SYBR® Green JumpStart™ Taq ReadyMix™ (Sigma) was used for both T and S qPCR. The final telomere primer concentrations were as follows: *tel 1*, 270 nM and *tel 2*, 900 nM. The final *36B4* (single copy gene) primer concentrations were *36B4u*, 300 nM and *36B4d*, 500 nM. Primer sequences (5' → 3') were as follows: *tel 1*, GGTTTTTGAGG GTGAGGGGTGAGGGTGTGAGGGTGTGAGGGT; *tel 2*, TCCCGACTATCC CTATCCCTATCCCTATCCCTATCCCTA; *36B4u*, CAGCAAGTGG GAAGGTGTAATCC; *36B4d*, CCCATTCTATCATCAACGGGTACAA (Mondello et al., 1999). All PCRs were performed using LightCycler® 480 by Roche thermocycler. For telomere PCR, 40 cycles of 95 °C for 15 s, 54 °C for 2 min, and for *36B4* PCR, 40 cycles of 95 °C for 15 s, 58 °C for 1 min were set. Telomere length LightCycler® 480 by Roche thermocycler was used to generate the standard curve for each run and to determine the dilution factors of standards corresponding to the T and S amounts in each sample. Absolute quantification results for both T and S were obtained using the Second Derivative Maximum method with the LightCycler® 480 Software v. 1.5. The relative telomere length value was expressed as the average of duplicate telomere over the average of duplicate single copy gene (T/S) ratio. All presented telomere length displayed as a relative level, compared to fibroblasts#1, passage 6. Standard deviation (s.d.) was obtained from three replicate values of each fibroblast sample, and statistical analysis was performed by Student's t test.

### CELL-IQ imaging

The early and late passage fibroblasts were taken into the Cell-IQ cell imaging system (ChipMan Technologies, Tampere, Finland) and visualized for 90 h to quantify the number of proliferative cells.

### Statistical analysis

To correlate the donor age and reprogramming efficiency we used linear regression carried out on reprogramming efficiency mean value ( $n = 4$ , two independent experiments) for donor fibroblasts ( $n = 11$ ) of various ages. Pearson's correlation coefficient and p value were calculated using Graph Pad Prism 6 software. Student t-test was used for statistical evaluation of iPSC reprogramming from early and late passage fibroblasts. A p value < 0.05 was considered statistically significant.

### Results and discussion

Pluripotency can be induced from somatic cells by the forced expression of the reprogramming factors OCT4, SOX2, KLF4

and c-MYC. To investigate the effects of donor ages on iPSC reprogramming, we studied human dermal fibroblasts from skin biopsies of 11 individuals representing different ages (0–83 years). The donors were either healthy volunteers or patients suffering from neonatal onset diabetes mellitus (PNDM) (Table 1). Although unlikely, we cannot exclude the possibility that the mutations causing PNDM may have had an effect on the reprogramming efficiency. The fibroblast outgrowths (passage 0) were cultured to establish cell lines for further experiments. Fibroblasts at early passage (p6) were transduced with retroviruses encoding OCT4, SOX2, KLF4 and c-MYC, and culture conditions were changed as shown (Fig. 1A). iPSC colonies emerged by day 10 after the induction (Fig. 1B). To compare iPSC-reprogramming efficiency among various donor ages (0–83 years), the emerging iPSC colonies with clear hESC morphology and positive for alkaline phosphatase (AP) staining were counted (Fig. 1B–D). Significantly, reprogramming efficiency correlated negatively and declined rapidly with increasing donor age (Fig. 1C and D).

We next asked what the impact of culture-induced senescence of the fibroblasts was on the reprogramming efficiency. Four representative fibroblast lines from young

(ages 0 and 1 year) and old (ages 81 and 83 year) donors were propagated for up to 25 passages (Fig. 2A). The pluripotent reprogramming efficiency of early and late passage fibroblasts was studied by counting AP-positive iPSC colonies with hESC-like morphology 21 days after the induction by non-integrating Sendai viral vectors. Regardless of donor age, early passage fibroblasts yielded significantly more iPSC colonies than late passage cells (Fig. 2B–D and Supplementary Fig. 2A). Similar to retroviral inductions, we observed the difference in reprogramming efficiencies of young (age 0, 1) and old fibroblasts (age 81, 83) when using Sendai viruses (Fig. 2C and D and Supplementary Fig. 2A).

Although the older fibroblasts gave only few iPSC colonies, the iPSC lines (HEL24.3 and HEL47.2) generated from neonatal and 83-year old donors, respectively (Trokovic et al., 2015), exhibited normal pluripotent stem cell properties, including the expression of the stem cell markers NANOG, TRA-1-60, OCT4, and SSEA3, as shown by immunocytochemistry (Supplementary Fig. 1A). All iPSC lines had activated the transcription of the endogenous pluripotency genes OCT4, SOX2, NANOG, and TDGF1 (Supplementary Fig. 1B). Both iPSC lines were negative for Sendai virus vectors as shown by

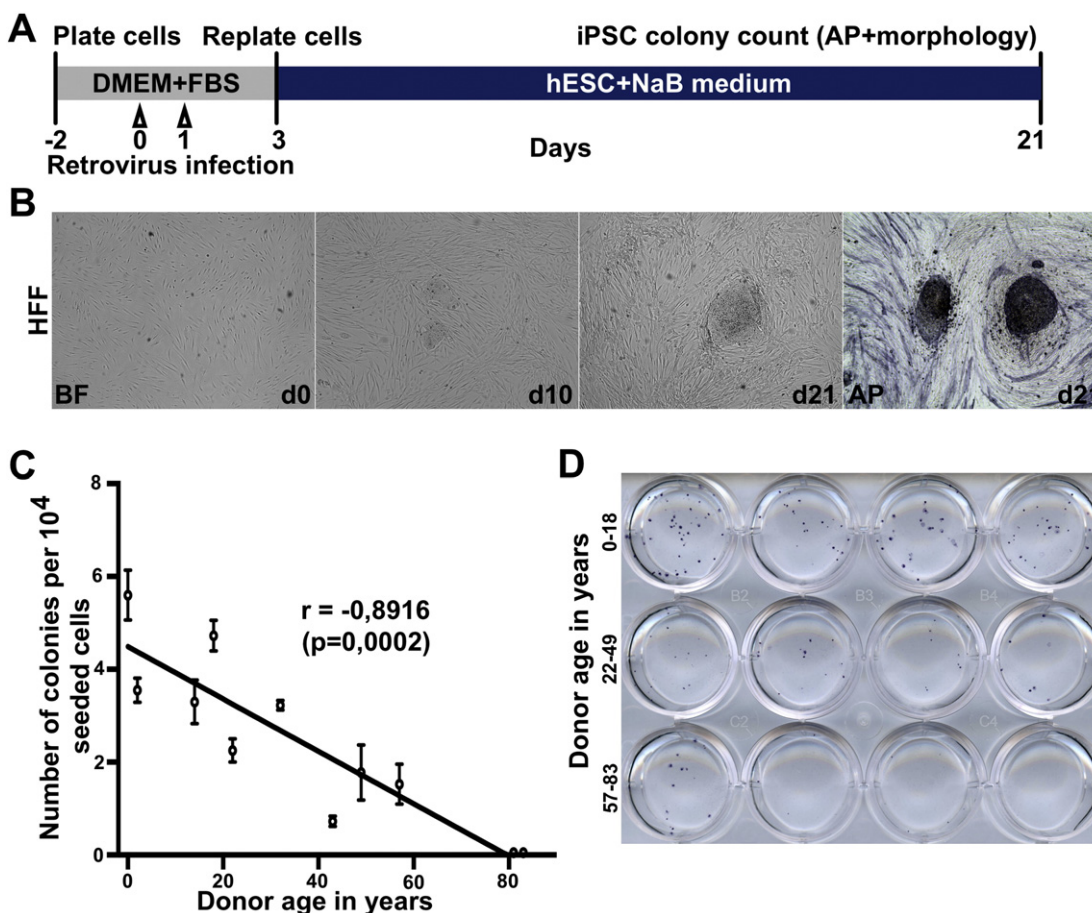


**Figure 1** Retroviral iPSC induction and characterization of the effect of donor age on reprogramming efficiency. A) Schematic presentation of iPSC induction using pMXs retroviruses. Fibroblasts were transduced at days 0 and 1, (arrowheads) prior to transferring to hESC culture conditions supplemented with sodium butyrate (NaB). B) Phase contrast images of representative fibroblasts (HFF) during the reprogramming process. Efficiency was calculated as the total number of iPSC colonies with hESC-like morphology positive for alkaline phosphatase (AP) at day 21. C) Correlation of reprogramming efficiency with donor age. The mean  $\pm$  SEM is shown for each sample (n = 4, two independent experiments). D) Representative images of AP staining for all donors at 21 days after start of induction.

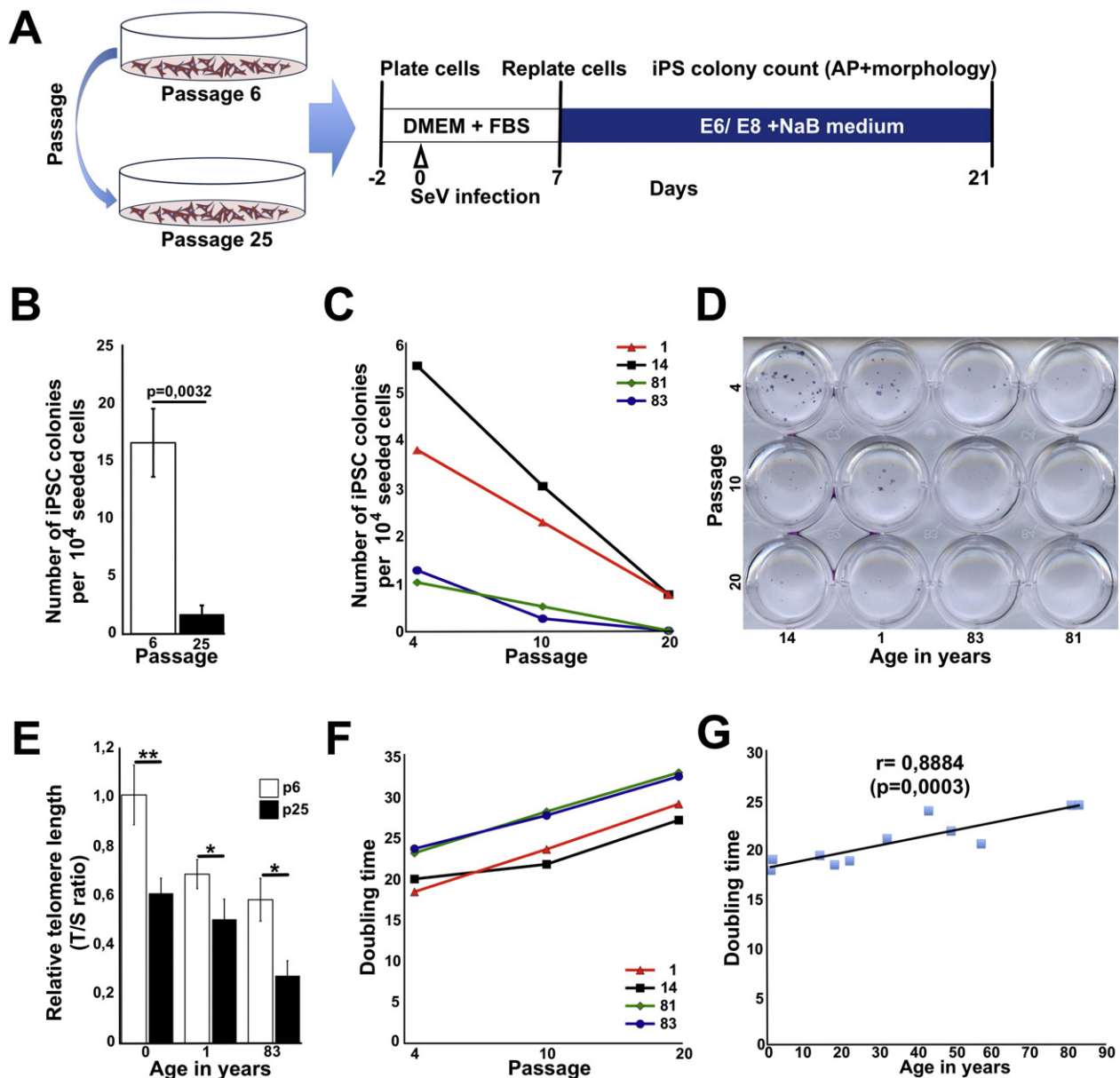


**Figure 2** Sendai virus iPS cell induction and characterization of the combined effect of donor age and passaging on reprogramming efficiency, telomere length and cell growth. A) Schematic presentation of the experimental protocol using Sendai viruses (SeV) for reprogramming. B) The effect of passage number (white column, p6; black column, p25) on reprogramming efficiency ( $n = 6$ ; from three independent fibroblast lines, Supplementary Fig. 2A.  $*p < 0.05$ ; Student's t-test). C) Combined effect of age and passage number on reprogramming efficiency of fibroblasts from 1-year (red), 14-year (black), 81-year (green), and 83-year (blue) old donors at passages 4, 10, and 20. D) Representative images of AP staining at day 21 after the start of induction shown for fibroblasts from 1-, 14-, 81-, and 83-year old donors at passages 4, 10 and 20. E) Telomere length of fibroblasts determined by quantitative PCR (qPCR) and presented as the relative telomere to single copy gene (T/S) ratio. Newborn fibroblasts at passage 6 were used as a reference sample. Passage 6 (white bars), passage 25 (black bars). Data are presented as mean  $\pm$  SD ( $n = 3$ ; three independent experiments.  $**p < 0.01$  and  $*p < 0.05$ ; Student's t-test). F) Doubling time of fibroblasts from 1-, 14-, 81-, and 83-year old donors measured at passages 4, 10, and 20. G) Correlation of doubling times with donor age. Pearson's correlation has been calculated for all fibroblasts at passage 6 ( $n = 3$ ).

immunocytochemistry and qPCR (Supplementary Fig. 1A and B). Multi-lineage differentiation capacity into all three-germ line lineages was demonstrated by teratoma formation (Supplementary Fig. 1C). Karyotype of iPSC line HEL24.3 (p14) was 46,XY and HEL47.2 (p14) 46,X, abn (Y). The

karyotype of the respective donor fibroblasts of HEL47.2 was also found to be 46,X, abn (Y).

Cellular aging in vitro was determined by cell proliferation and telomere length. Telomere length, which has been associated with human aging (Marion et al., 2009), was

significantly shortened by prolonged culture of all fibroblasts (Fig. 2E). In accordance with telomere length, proliferation rate of the fibroblasts, examined by live-cell imaging, was reduced in all long-term cultured samples (Fig. 2F and Supplementary Fig. 2B). With increasing time in culture, the population doubling times of fibroblasts from 0 and 1-year old donors increased from 18 to 20 and 18 to 33 h, respectively. Similarly, fibroblasts from the 83-year old donor showed a marked elongation of doubling time, from 21 to 33 h. We then assessed the proliferation rate of all donor fibroblast lines, at passages 6–8, and observed a significant positive correlation between increasing age and doubling time (Fig. 2G).

To uncover the possible mechanisms underlying the differences in reprogramming efficiency, expression of selected genes controlling cell cycle and apoptosis were investigated. The genes were selected based on previous reports of their role in iPSC reprogramming (Hong et al., 2009; Li et al., 2013). In mammalian cells, permanent growth arrest is achieved through one of the two signaling pathways p53/p21 and p16/Rb (Choudhury et al., 2007; Wright and Shay, 1992). Notably, p21 was dramatically upregulated in long term-cultured fibroblasts, while there was no change in p16, p53 or PUMA expression (Fig. 3A). Besides the upregulation of p21, long term-cultured fibroblasts displayed significant shortening of telomeres (Fig. 2E). This observation was in line with the role of p21 in mediating senescence in response to telomere dysfunction (Brown et al., 1997). As p21 inhibition has been demonstrated to enhance reprogramming efficiency predominantly by the cell division rate-dependent mechanisms (Hanna et al., 2009), it is likely that the reduction of cell proliferation and reprogramming efficiency coinciding with the increase in p21 expression are mechanistically related in reducing reprogramming efficiency. Our data show that both donor age and passage number are strongly correlated with increasing p21 expression (Fig. 3B and C), indicating cellular senescence-induced upregulation of p21.

Our results are in line with previous findings showing that cellular senescence negatively correlates with reprogramming efficiency (Banito et al., 2009; Mali et al., 2008; Qin et al., 2007; Zhao and Daley, 2008; Zhao et al., 2008). The expression of p21 is controlled by p53 during the replicative senescence of normal human fibroblasts (Jackson and Pereira-Smith, 2006). It has been shown that the inhibitory effects of senescence on

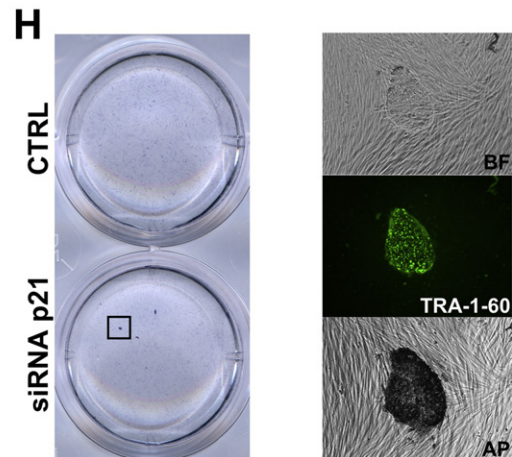
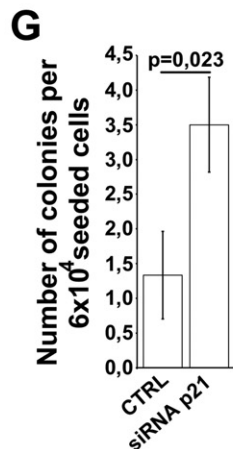
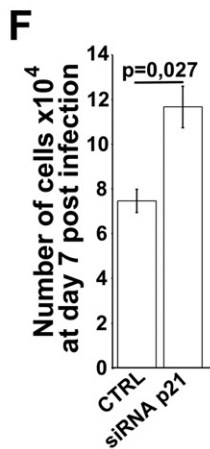
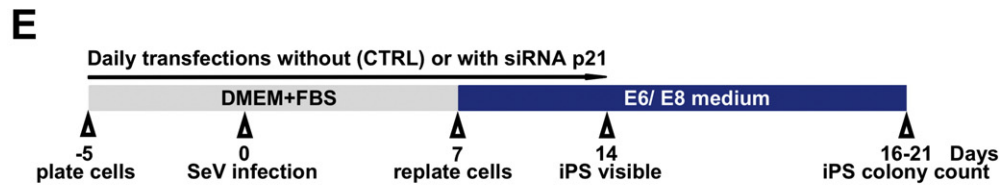
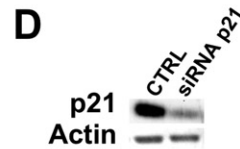
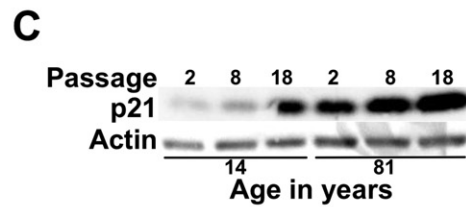
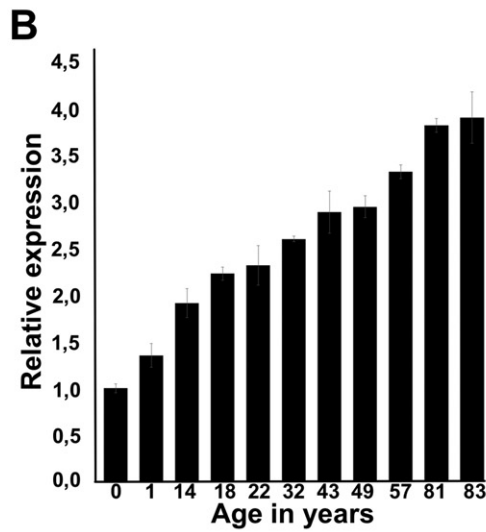
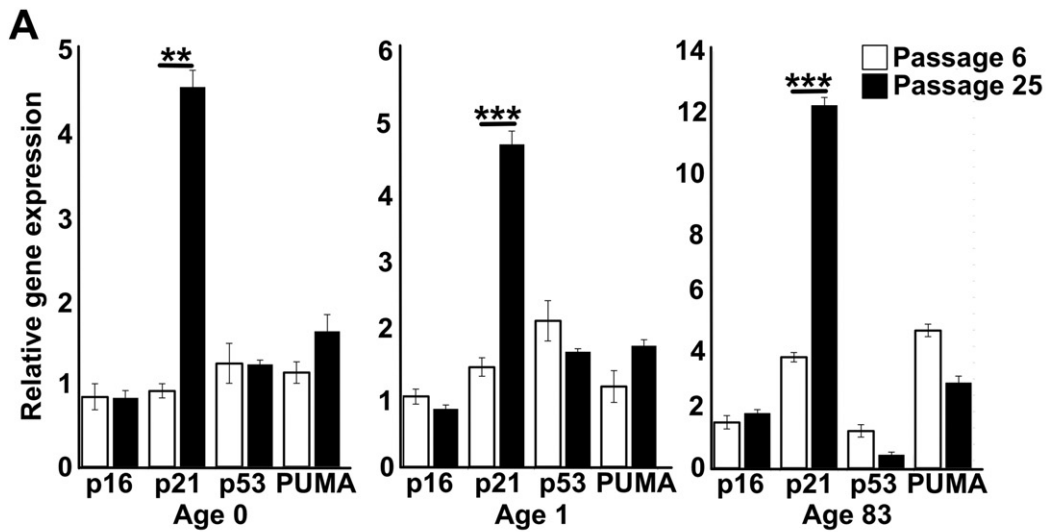
reprogramming can be overcome by inhibition of p53 pathway (Banito et al., 2009; Hong et al., 2009; Kawamura et al., 2009; Li et al., 2009; Rasmussen et al., 2014; Utikal et al., 2009; Zhao et al., 2008). In addition, supplementing reprogramming media with vitamin C has been shown to significantly improve the reprogramming efficiency of senescent cells (Esteban et al., 2010).

Next we wanted to determine if we could rescue the reprogramming efficiency of late passage (p28) fibroblasts from young (0 and 1-year) and old (81 and 83-year) donors by inhibiting the p53/p21 pathway by siRNA-mediated knockdown of p21. First we verified that the siRNA against p21 was indeed able to strongly reduce the P21 protein level in passaged fibroblasts (Fig. 3D). To alleviate senescence in passaged fibroblasts we started transfections of siRNA against p21 five days prior to reprogramming. Daily transfections continued until day 14, when we were able to visualize newly formed iPSC colonies (Fig. 3E). The addition of p21 siRNA significantly increased the number of fibroblasts during the first days of reprogramming (Fig. 3F). The pluripotent reprogramming efficiency of late passage fibroblasts was studied by counting AP-positive iPSC colonies with hESC-like morphology, and live staining for stem cell surface marker TRA-1-60, 16–21 days after the induction. Knockdown of p21 was able to rescue the reprogramming efficiency of late passage fibroblasts derived from all donors (Fig. 3G and H and Supplementary Fig. 3A and B). This is in striking contrast to the standard condition in which no iPSC colonies were detected from old (81 and 83-year) donor fibroblasts.

Finally, in order to show conclusively that p21 directly controls reprogramming efficiency, we overexpressed p21 for the entire duration of the experiment in fibroblasts from 0 and 1-year old donors at passages 7 and 2 respectively (Supplementary Fig. 3D). Overexpression of p21 resulted in suppression of growth of transfected fibroblasts, which was expected based on the previous reports (el-Deiry et al., 1993; Harper et al., 1995; Xiong et al., 1993), and no iPSC colonies were generated (Supplementary Fig. 3E and F).

In conclusion, our results demonstrate that fibroblasts obtained from both young and old donors can give rise to iPSC. However, young and early passage fibroblasts yield the highest reprogramming efficiency, while advanced donor age and time in culture induce a synergistic negative effect

**Figure 3** Effect of the cell cycle inhibitor p21 on reprogramming efficiency in passaged fibroblasts A) Significant upregulation of *CDKN1A* (p21) mRNA levels in long term-cultured fibroblasts (passage 25) ( $n = 3$ ; three independent experiments.  $***p < 0.001$ ,  $**p < 0.01$ ; Student's t-test). B) Relative expression of *CDKN1A* (p21) for all fibroblasts (age 0–83) at passage 6 ( $n = 3$ ). Relative expression levels were measured by qPCR, and fold changes were calculated relative to neonatal fibroblasts at passage 6, after normalization to *Cyclophilin G*. C) Western blot analysis of p21 protein levels from the fibroblasts of 14-year old and 81-year old donors at passages 2, 8, and 18. D) Knockdown of p21 by siRNA. Western blot of p21 for neonatal fibroblasts at passage 20. CTRL, control; siRNA p21, passage 20 cells treated with siRNA against p21 for 72 h. E) Schematic presentation of p21 knockdown experiment. Fibroblasts were transfected without vector (CTRL) or with siRNA against p21 on a daily basis, starting five days prior to SeV infection and lasting until iPSC colonies were clearly visible (day 14). F) Effect of p21 knockdown (siRNAp21) on the growth of late passage fibroblasts. Data presented is combined from 0-, 81-, and 83-year old donor fibroblasts at passage 25 ( $N = 3$ ). The cells were counted at days 0 and 7. G) Effect of p21 knockdown (siRNAp21) on the reprogramming efficiency of late passage fibroblasts (combined from 0-, 1-, 81-, and 83-year old donors, passage 25,  $N = 4$ ). Reprogramming efficiencies for each line are shown in Supplementary Fig. 3B. H) Representative image of AP staining at day 21 after the start of induction of fibroblasts at passage 25 comparing to p21 knockdowns with untreated control. Panels on the right show TRA-1-60 and AP staining of the same iPSC colony, enlarged from picture H (black square). Bright field (BF), TRA-1-60 (green), alkaline phosphatase (AP). Data for all passage 25 fibroblast donors (0-, 1-, 81-, and 83-year old) is shown in Supplementary Fig. 3A and B.



markedly reducing the number of iPSC colonies. The negative effect of donor age and time in culture on reprogramming efficiency appears to be associated with cellular senescence mediated primarily by upregulation of the cell cycle inhibitory protein p21. Our results demonstrate that iPSC generation can be enhanced even from late passage human fibroblasts from old donors through inhibition of p21 during the reprogramming process.

Supplementary data to this article can be found online at <http://dx.doi.org/10.1016/j.scr.2015.06.001>.

## Acknowledgments

This work was supported by grants from the Academy of Finland (No. 257157, 250890 to P.N., 251413 to T.R.), Foundation for Pediatric Research (7495 to T.R.), the Sigrid Jusélius Foundation (2613 to T.R.) and the research funds of the Helsinki University Central Hospital (TYH2012302, TYH2014408 to T.R.). SeVdp vector was produced and kindly provided by Prof. Mahito Nakanishi ([mahito-nakanishi@aist.go.jp](mailto:mahito-nakanishi@aist.go.jp)) from the National Institute of Advanced Industrial Science and Technology (AIST). The authors are grateful to Elina Hakonen for critically reading the manuscript and helping with statistical analysis, to Heli Mononen for help with Cell-IQ experiment and to Jarkko Ustinov for derivation of primary fibroblast lines.

## References

- Banito, A., Rashid, S.T., Acosta, J.C., Li, S., Pereira, C.F., Geti, I., Pinho, S., Silva, J.C., Azuara, V., Walsh, M., Vallier, L., Gil, J., 2009. Senescence impairs successful reprogramming to pluripotent stem cells. *Genes Dev.* 23 (18), 2134–2139.
- Braam, S.R., Tertoolen, L., Casini, S., Matsa, E., Lu, H.R., Teisman, A., Passier, R., Denning, C., Gallacher, D.J., Towart, R., Mummery, C.L., 2013. Repolarization reserve determines drug responses in human pluripotent stem cell derived cardiomyocytes. *Stem Cell Res.* 10 (1), 48–56.
- Brown, J.P., Wei, W., Sedivy, J.M., 1997. Bypass of senescence after disruption of p21CIP1/WAF1 gene in normal diploid human fibroblasts. *Science* 277 (5327), 831–834.
- Campisi, J., d'Adda di Fagagna, F., 2007. Cellular senescence: when bad things happen to good cells. *Nat. Rev. Mol. Cell Biol.* 8 (9), 729–740.
- Cawthon, R.M., 2002. Telomere measurement by quantitative PCR. *Nucleic Acids Res.* 30 (10), e47.
- Choudhury, A.R., Ju, Z., Djojotubroto, M.W., Schienke, A., Lechel, A., Schaetzlein, S., Jiang, H., Stepczynska, A., Wang, C., Buer, J., Lee, H.W., von Zglinicki, T., Ganser, A., Schirmacher, P., Nakauchi, H., Rudolph, K.L., 2007. Cdkn1a deletion improves stem cell function and lifespan of mice with dysfunctional telomeres without accelerating cancer formation. *Nat. Genet.* 39 (1), 99–105.
- el-Deiry, W.S., Tokino, T., Velculescu, V.E., Levy, D.B., Parsons, R., Trent, J.M., Lin, D., Mercer, W.E., Kinzler, K.W., Vogelstein, B., 1993. WAF1, a potential mediator of p53 tumor suppression. *Cell* 75 (4), 817–825.
- Eminli, S., Foudi, A., Stadtfeld, M., Maherali, N., Ahfeldt, T., Mostoslavsky, G., Hock, H., Hochedlinger, K., 2009. Differentiation stage determines potential of hematopoietic cells for reprogramming into induced pluripotent stem cells. *Nat. Genet.* 41 (9), 968–976.
- Esteban, M.A., Wang, T., Qin, B., Yang, J., Qin, D., Cai, J., Li, W., Weng, Z., Chen, J., Ni, S., Chen, K., Li, Y., Liu, X., Xu, J., Zhang, S., Li, F., He, W., Labuda, K., Song, Y., Peterbauer, A., Wolbank, S., Redl, H., Zhong, M., Cai, D., Zeng, L., Pei, D., 2010. Vitamin C enhances the generation of mouse and human induced pluripotent stem cells. *Cell Stem Cell* 6 (1), 71–79.
- Hanna, J., Saha, K., Pando, B., van Zon, J., Lengner, C.J., Creighton, M.P., van Oudenaarden, A., Jaenisch, R., 2009. Direct cell reprogramming is a stochastic process amenable to acceleration. *Nature* 462 (7273), 595–601.
- Harper, J.W., Elledge, S.J., Keyomarsi, K., Dynlacht, B., Tsai, L.H., Zhang, P., Dobrowolski, S., Bai, C., Connell-Crowley, L., Swindell, E., et al., 1995. Inhibition of cyclin-dependent kinases by p21. *Mol. Biol. Cell* 6 (4), 387–400.
- Hong, H., Takahashi, K., Ichisaka, T., Aoi, T., Kanagawa, O., Nakagawa, M., Okita, K., Yamanaka, S., 2009. Suppression of induced pluripotent stem cell generation by the p53–p21 pathway. *Nature* 460 (7259), 1132–1135.
- Hou, P., Li, Y., Zhang, X., Liu, C., Guan, J., Li, H., Zhao, T., Ye, J., Yang, W., Liu, K., Ge, J., Xu, J., Zhang, Q., Zhao, Y., Deng, H., 2013. Pluripotent stem cells induced from mouse somatic cells by small-molecule compounds. *Science* 341 (6146), 651–654.
- Hussein, S.M., Batada, N.N., Vuoristo, S., Ching, R.W., Autio, R., Narva, E., Ng, S., Sourour, M., Hamalainen, R., Olsson, C., Lundin, K., Mikkola, M., Trokovic, R., Peitz, M., Brustle, O., Bazett-Jones, D.P., Alitalo, K., Lahesmaa, R., Nagy, A., Otonkoski, T., 2011. Copy number variation and selection during reprogramming to pluripotency. *Nature* 471 (7336), 58–62.
- Jackson, J.G., Pereira-Smith, O.M., 2006. p53 is preferentially recruited to the promoters of growth arrest genes p21 and GADD45 during replicative senescence of normal human fibroblasts. *Cancer Res.* 66 (17), 8356–8360.
- Kawamura, T., Suzuki, J., Wang, Y.V., Menendez, S., Morera, L.B., Raya, A., Wahl, G.M., Belmonte, J.C., 2009. Linking the p53 tumour suppressor pathway to somatic cell reprogramming. *Nature* 460 (7259), 1140–1144.
- Lapasset, L., Milhavel, O., Prieur, A., Besnard, E., Babled, A., Ait-Hamou, N., Leschik, J., Pellestor, F., Ramirez, J.M., De Vos, J., Lehmann, S., Lemaitre, J.M., 2011. Rejuvenating senescent and centenarian human cells by reprogramming through the pluripotent state. *Genes Dev.* 25 (21), 2248–2253.
- Li, H., Collado, M., Villasante, A., Strati, K., Ortega, S., Canamero, M., Blasco, M.A., Serrano, M., 2009. The Ink4/Arf locus is a barrier for iPSC cell reprogramming. *Nature* 460 (7259), 1136–1139.
- Li, Y., Feng, H., Gu, H., Lewis, D.W., Yuan, Y., Zhang, L., Yu, H., Zhang, P., Cheng, H., Miao, W., Yuan, W., Cheng, S.Y., Gollin, S.M., Cheng, T., 2013. The p53-PUMA axis suppresses iPSC generation. *Nat. Commun.* 4, 2174.
- Mali, P., Ye, Z., Hommond, H.H., Yu, X., Lin, J., Chen, G., Zou, J., Cheng, L., 2008. Improved efficiency and pace of generating induced pluripotent stem cells from human adult and fetal fibroblasts. *Stem Cells* 26 (8), 1998–2005.
- Marión, R.M., Strati, K., Li, H., Murga, M., Blanco, R., Ortega, S., Fernandez-Capetillo, O., Serrano, M., Blasco, M.A., 2009. A p53-mediated DNA damage response limits reprogramming to ensure iPSC cell genomic integrity. *Nature* 460 (7259), 1149–1153.
- Marion, R.M., Strati, K., Li, H., Tejera, A., Schoeftner, S., Ortega, S., Serrano, M., Blasco, M.A., 2009. Telomeres acquire embryonic stem cell characteristics in induced pluripotent stem cells. *Cell Stem Cell* 4 (2), 141–154.
- Mondello, C., Petropoulou, C., Monti, D., Gonos, E.S., Franceschi, C., Nuzzo, F., 1999. Telomere length in fibroblasts and blood cells from healthy centenarians. *Exp. Cell Res.* 248 (1), 234–242.
- Narita, M., Nunez, S., Heard, E., Narita, M., Lin, A.W., Hearn, S.A., Spector, D.L., Hannon, G.J., Lowe, S.W., 2003. Rb-mediated heterochromatin formation and silencing of E2F target genes during cellular senescence. *Cell* 113 (6), 703–716.
- Nishimura, K., Sano, M., Ohtaka, M., Furuta, B., Umemura, Y., Nakajima, Y., Ikehara, Y., Kobayashi, T., Segawa, H., Takayasu,



- S., Sato, H., Motomura, K., Uchida, E., Kanayasu-Toyoda, T., Asashima, M., Nakauchi, H., Yamaguchi, T., Nakanishi, M., 2011. Development of defective and persistent Sendai virus vector: a unique gene delivery/expression system ideal for cell reprogramming. *J. Biol. Chem.* 286 (6), 4760–4771.
- Park, S.J., Yeo, H.C., Kang, N.Y., Kim, H., Lin, J., Ha, H.H., Vendrell, M., Lee, J.S., Chandran, Y., Lee, D.Y., Yun, S.W., Chang, Y.T., 2014. Mechanistic elements and critical factors of cellular reprogramming revealed by stepwise global gene expression analyses. *Stem Cell Res.* 12 (3), 730–741.
- Qin, H., Yu, T., Qing, T., Liu, Y., Zhao, Y., Cai, J., Li, J., Song, Z., Qu, X., Zhou, P., Wu, J., Ding, M., Deng, H., 2007. Regulation of apoptosis and differentiation by p53 in human embryonic stem cells. *J. Biol. Chem.* 282 (8), 5842–5852.
- Rasmussen, M.A., Holst, B., Tumer, Z., Johnsen, M.G., Zhou, S., Stummann, T.C., Hyttel, P., Clausen, C., 2014. Transient p53 suppression increases reprogramming of human fibroblasts without affecting apoptosis and DNA damage. *Stem Cell Rep.* 3 (3), 404–413.
- Seki, T., Yuasa, S., Oda, M., Egashira, T., Yae, K., Kusumoto, D., Nakata, H., Tohyama, S., Hashimoto, H., Kodaira, M., Okada, Y., Seimiya, H., Fusaki, N., Hasegawa, M., Fukuda, K., 2010. Generation of induced pluripotent stem cells from human terminally differentiated circulating T cells. *Cell Stem Cell* 7 (1), 11–14.
- Smith, Z.D., Nachman, I., Regev, A., Meissner, A., 2010. Dynamic single-cell imaging of direct reprogramming reveals an early specifying event. *Nat. Biotechnol.* 28 (5), 521–526.
- Somers, A., Jean, J.C., Sommer, C.A., Omari, A., Ford, C.C., Mills, J.A., Ying, L., Sommer, A.G., Jean, J.M., Smith, B.W., Lafyatis, R., Demierre, M.F., Weiss, D.J., French, D.L., Gadue, P., Murphy, G.J., Mostoslavsky, G., Kotton, D.N., 2010. Generation of transgene-free lung disease-specific human induced pluripotent stem cells using a single excisable lentiviral stem cell cassette. *Stem Cells* 28 (10), 1728–1740.
- Song, B., Sun, G., Herszfeld, D., Sylvain, A., Campanale, N.V., Hirst, C.E., Caine, S., Parkington, H.C., Tonta, M.A., Coleman, H.A., Short, M., Ricardo, S.D., Reubinoff, B., Bernard, C.C., 2012. Neural differentiation of patient specific iPSC cells as a novel approach to study the pathophysiology of multiple sclerosis. *Stem Cell Res.* 8 (2), 259–273.
- Streckfuss-Bomeke, K., Wolf, F., Azizian, A., Stauske, M., Tiburcy, M., Wagner, S., Hubscher, D., Dressel, R., Chen, S., Jende, J., Wulf, G., Lorenz, V., Schon, M.P., Maier, L.S., Zimmermann, W.H., Hasenfuss, G., Guan, K., 2013. Comparative study of human-induced pluripotent stem cells derived from bone marrow cells, hair keratinocytes, and skin fibroblasts. *Eur. Heart J.* 34 (33), 2618–2629.
- Takahashi, K., Yamanaka, S., 2006. Induction of pluripotent stem cells from mouse embryonic and adult fibroblast cultures by defined factors. *Cell* 126 (4), 663–676.
- Takahashi, K., Tanabe, K., Ohnuki, M., Narita, M., Ichisaka, T., Tomoda, K., Yamanaka, S., 2007. Induction of pluripotent stem cells from adult human fibroblasts by defined factors. *Cell* 131 (5), 861–872.
- Trokovic, R., Weltner, J., Manninen, T., Mikkola, M., Lundin, K., Hamalainen, R., Suomalainen, A., Otonkoski, T., 2013. Small molecule inhibitors promote efficient generation of induced pluripotent stem cells from human skeletal myoblasts. *Stem Cells Dev.* 22 (1), 114–123.
- Trokovic, R., Weltner, J., Nishimura, K., Ohtaka, M., Nakanishi, M., Salomaa, V., Jalanko, A., Otonkoski, T., Kyttala, A., 2014. Advanced feeder-free generation of induced pluripotent stem cells directly from blood cells. *Stem Cells Transl. Med.* 12, 1402–1409.
- Trokovic, R., Weltner, J., Otonkoski, T., 2015. Generation of iPSC line HEL24.3 from human neonatal foreskin fibroblasts. *Stem Cell Res.* 15, 266–268.
- Trokovic, R., Weltner, J., Otonkoski, T., 2015. Generation of iPSC line HEL47.2 from healthy human adult fibroblasts. *Stem Cell Res.* 15, 263–265.
- Utikal, J., Polo, J.M., Stadtfeld, M., Maherali, N., Kulalert, W., Walsh, R.M., Khalil, A., Rheinwald, J.G., Hochedlinger, K., 2009. Immortalization eliminates a roadblock during cellular reprogramming into iPSCs. *Nature* 460 (7259), 1145–1148.
- Wang, B., Miyagoe-Suzuki, Y., Yada, E., Ito, N., Nishiyama, T., Nakamura, M., Ono, Y., Motohashi, N., Segawa, M., Masuda, S., Takeda, S., 2011. Reprogramming efficiency and quality of induced Pluripotent Stem Cells (iPSCs) generated from muscle-derived fibroblasts of mdx mice at different ages. *PLoS Curr.* 3, RRN1274.
- Warren, L., Manos, P.D., Ahfeldt, T., Loh, Y.H., Li, H., Lau, F., Ebina, W., Mandal, P.K., Smith, Z.D., Meissner, A., Daley, G.Q., Brack, A.S., Collins, J.J., Cowan, C., Schlaeger, T.M., Rossi, D.J., 2010. Highly efficient reprogramming to pluripotency and directed differentiation of human cells with synthetic modified mRNA. *Cell Stem Cell* 7 (5), 618–630.
- Wright, W.E., Shay, J.W., 1992. Telomere positional effects and the regulation of cellular senescence. *Trends Genet.* 8 (6), 193–197.
- Xiong, Y., Hannon, G.J., Zhang, H., Casso, D., Kobayashi, R., Beach, D., 1993. p21 is a universal inhibitor of cyclin kinases. *Nature* 366 (6456), 701–704.
- Yu, J., Vodyanik, M.A., Smuga-Otto, K., Antosiewicz-Bourget, J., Frane, J.L., Tian, S., Nie, J., Jonsdottir, G.A., Ruotti, V., Stewart, R., Slukvin, I.I., Thomson, J.A., 2007. Induced pluripotent stem cell lines derived from human somatic cells. *Science* 318 (5858), 1917–1920.
- Yu, Y., Liu, H., Ikeda, Y., Amiot, B.P., Rinaldo, P., Duncan, S.A., Nyberg, S.L., 2012. Hepatocyte-like cells differentiated from human induced pluripotent stem cells: relevance to cellular therapies. *Stem Cell Res.* 9 (3), 196–207.
- Zhao, R., Daley, G.Q., 2008. From fibroblasts to iPSCs: induced pluripotency by defined factors. *J. Cell. Biochem.* 105 (4), 949–955.
- Zhao, Y., Yin, X., Qin, H., Zhu, F., Liu, H., Yang, W., Zhang, Q., Xiang, C., Hou, P., Song, Z., Liu, Y., Yong, J., Zhang, P., Cai, J., Liu, M., Li, H., Li, Y., Qu, X., Cui, K., Zhang, W., Xiang, T., Wu, Y., Zhao, Y., Liu, C., Yu, C., Yuan, K., Lou, J., Ding, M., Deng, H., 2008. Two supporting factors greatly improve the efficiency of human iPSC generation. *Cell Stem Cell* 3 (5), 475–479.
- Zhou, H., Wu, S., Joo, J.Y., Zhu, S., Han, D.W., Lin, T., Trauger, S., Bien, G., Yao, S., Zhu, Y., Siuzdak, G., Scholer, H.R., Duan, L., Ding, S., 2009. Generation of induced pluripotent stem cells using recombinant proteins. *Cell Stem Cell* 4 (5), 381–384.